Smart Materials in Medicine 4 (2023) 123–133

Contents lists available at ScienceDirect

Smart Materials in Medicine

journal homepage: www.keaipublishing.com/en/journals/smart-materials-in-medicine/

# A study involving PC-3 cancer cells and novel carbamate gemini surfactants: Is zeta potential the key to control adhesion to cells?

R.V. Pavlov *, G.A. Gaynanova, D.M. Kuznetsov, Ya.A. Ivanov, S.K. Amerkhanova, A.P. Lyubina, A.D. Voloshina, L.Ya. Zakharova

*Arbuzov Institute of Organic and Physical Chemistry, FRC Kazan Scientific Center, Russian Academy of Sciences, 8 Arbuzov str, 420088, Kazan, Russian Federation*

ARTICLE INFO

*Keywords:*
Cationic liposome
PC-3
Cellular uptake
RGD
Zeta potential

ABSTRACT

Liposome surface potential effect on cellular uptake and cytotoxicity is evaluated using liposomes, modified with cationic lipid DOTAP, a series of cationic gemini surfactants with two carbamate fragments, and an amphiphilic peptide SSRGD. The surfactants used are novel representatives of the gemini family with improved self-assembling activity coupled with potential biodegradable properties and displayed increasing antibacterial activity and cytotoxicity with the shortening of hydrophobic alkyl tails. The longest alkyl tail surfactant, 14-6-14(Et), was the most biocompatible of the series, which was chosen for liposome modification. Prepared liposomes of various compositions are characterized from morphological and physicochemical standpoints in order to optimize their biocompatibility and stability. The carbamate gemini surfactants were also twice as effective at providing positive charge to liposomes and less toxic compared to DOTAP. On their own, carbamate surfactants were able to increase cellular uptake of liposomes by 190%. The mixed composition of 14-6-14(Et) surfactant and SSRGD amphiphilic peptide was the most readily absorbed formulation among different tested neutral, cationic and RGD-modified liposomes. The comparison between the cellular uptake promotion is conducted as to what is the most selective and efficient approach to enhance lipid nanoparticle uptake by cancerous cells.

## 1. Introduction

A lot of research attention is currently attracted to nanomedicine. Nanoparticle-based formulations of drugs and other therapeutic agents such as genetic material exhibit higher efficiency and lower adverse effects [1–4]. All of the nanosized formulations undergo interactions with various cell membranes in the body [5]. These interactions are often key to the specific advantages of using one nanocontainer over the other and can decide whether a particular nanomedical approach can be successful [6,7].

One of the fundamental parameters dictating nanoparticle-cell interactions is their charge. Despite a large number of papers discussing the effect of particle charge present to this date, overall understanding of what should the particle charge be for anticancer nanomedicine is not yet reached [8]. Many results are contradictory and not comparable with each other due to differences in cell types, particles, and experimental approaches. Uptake of cationic or anionic particles sometimes differs depending on the cell type, which allows to target liposomes to certain cells with their charge [9,10]. For the delivery of genetic material cationic particles are generally considered optimal primarily because of their ability to store and protect negatively charged nucleic acids [11]. Generalization of the role of particle charge is further complicated by a diversity of cells cultures and nanoparticle types, which can have different morphology, sizes, and specific interactions with cell receptors. Research of liposome uptake mechanisms by cells is ongoing [12] and one of the recent studies concludes that the primary uptake mechanism for both cationic and anionic particles is micropinocytosis [13]. There is also evidence that uptake intensity and mechanism could be strongly affected by stereochemistry of gemini cationic surfactants used to modify liposomes [14,15]. Other research suggests that primary mechanism of uptake for cationic nanoparticles is charge-mediated adsorption and consequent endocytosis (adsorptive endocytosis) [16]. In the brain drug delivery literature it is well-established that cationic nanoparticles enhance cellular association and endothelial layer penetration via electrostatic adsorption initially, referring to this process as adsorption-mediated transcytosis [17–20]. Furthermore, in the bloodstream, particles with a strong charge, positive or negative, collect protein corona and are more easily absorbed by the reticuloendothelial system [21–23]. From a physicochemical standpoint, the driving force of

* Corresponding author.
*E-mail address:* rais.pavlov@iopc.ru (R.V. Pavlov).

https://doi.org/10.1016/j.smaim.2022.09.001
Received 31 July 2022; Received in revised form 1 September 2022; Accepted 5 September 2022
Available online 12 September 2022

**Abbreviations:**

| | |
|---|---|
| n-s-n(Et) | carbamate gemini surfactants (N,N′-dialkyl-N,N′-bis (2-(ethylcarbamoyloxy)ethyl)-N,N′-dimethylhexane-1,6-diammonium dibromide) |
| DOX | doxorubicin |
| C6 | coumarin 6 |
| SSRGD | amphiphilic peptide N-palmitoyl-Ser-Ser-Arg-Gly-Asp |
| DOTAP | 1,2-dioleoyl-3-trimethylammonium propane |
| CMC | critical micelle concentration |
| PdI | polydispersity index |
| ZP | zeta potential |

association of cationic particles with negative cellular membranes is Coulomb attraction. In this work, an attempt is made to correlate zeta potential – a measure of particle's response to electric field, and cell association and uptake – quantified by flow cytometry.

PC-3, a human prostate carcinoma cell line was many times used to study efficacy of cationic liposomes as delivery vehicles for chemotherapy or nucleic acids [24–28]. Cationic liposomes were shown to passively accumulate in tumor tissues, and tumor cells also have a more negative membrane potential than healthy ones [28–30]. These cells also overexpress $\alpha_5\beta_1$ and $\alpha_v\beta_3$ integrins [31] that can be targeted by an RGD peptide motif [32,33]. PC-3 can be a good object to characterize effects of liposome charge and compare them to RGD-mediated binding.

An efficient method of cationizing liposomes is incorporation of cationic surfactants, among which the gemini surfactants have attracted a lot of attention in the past, due to multiple unique properties, such as efficient complexation with nucleic acids [34], interaction with the bilayer (affecting lipid bilayer phase transition temperature) [35], enantiomer-dependent aggregation [36], pH or light induced switchable aggregation [37]. Comprehensive research of novel biocompatible gemini surfactants is ongoing [38–43], as well as thorough reviews on their biomedical and anti-corrosive properties are published [44,45], which indicates hidden potential in the gemini surfactants that is yet to be discovered. From the biomedical standpoint, gemini surfactants are, first of all, known as transfection agents [35]. A lot of research focuses on their good ability to form lipoplexes via self-assembly with DNA and RNA [11,46–48]. As surfactants, geminis have lower aggregation thresholds and higher solubilizing capacities compared to conventional alkylammonium surfactants.

In our group, it was previously shown that cationic hydroxyethyl gemini surfactants were able to impart blood-brain barrier penetrating properties to liposomes as an oxime therapy for organophosphate poisoning [49]. As a follow-up, a biodegradable carbamate function was added to the surfactant structure to facilitate complex intermolecular interactions for self-assembly. These surfactants are then used to impart a cationic charge to liposomes, which can be done at lower concentrations than with mono-cationic surfactants or lipids, preserving the integrity of the lipid bilayer and not reaching highly cytotoxic concentrations. In this work, synthesis and aggregation properties of carbamate gemini surfactants are characterized, and they are compared with a cationic lipid DOTAP and cellular adhesion peptide RGD in ability to enhance liposome interactions with cells. With these objects the contribution can be made towards generalization of the effects of liposome zeta potential on association with PC-3 cells, as well as the effects of the charge can be compared to those of RGD.

## 2. Materials and methods

$H_2O$ Milli-Q was purified with Millipore Direct-Q 5 UV system. Pyrene, 99%, coumarin 6 (C6), >99%, cholesterol (Chol), 99%, HEPES, >99.5%, were obtained from Sigma-Aldrich. Orange OT, 70% dye content, was supplied by ChemCruz (USA). Dioleoyl-3-trimethylammonium propane (DOTAP) was a gift from Lipoid (Ludwigshafen, Germany), soybean phosphatidylcholine (PC) 95% was obtained from Avanti (USA). The amphiphilic peptide with a hexadecyl alkyl tail SSRGD-16 (SSRGD), >95%, was sourced from Almabion (Russia). N,N′-dialkyl-N,N′-bis (2-(ethylcarbamoyloxy)ethyl)-N,N′-dimethylhexane-1,6-diammonium dibromide (10-6-10(Et), 12-6-12(Et), 14-6-14(Et)) were synthesized from the hydroxyethyl gemini as described below (Fig. 1). The precursor synthesis is described in Refs. [50,51].

### 2.1. Synthesis of gemini surfactants with a carbamate fragment

General procedure. The mixture of 1 eq of N,N′-dialkyl-N,N′-bis(2-hydroxyethyl)-N,N′-dimethylhexane-1,6-diammonium dibromide, 0.05 g DABCO (1,4-Diazabicyclo[2.2.2]octane) and 4 eq ethyl isocyanate was stirred in 20 mL dry acetonitrile at 60 °C during 16 h. A white precipitate formed in the reaction mixture, which was filtered and recrystallized from ethyl acetate. The precipitate was filtered and dried on a water bath (45 °C) under vacuum (15 mm Hg). Details are provided in the supplementary material, NMR, FTIR, ESI spectra are shown in Figs. S1–S9.

### 2.2. Tensiometry

Tensiometric measurements were carried out on a Kruss K6 tensiometer (Germany), based on the Du-Nuoy ring detachment method. For the experiment, a series of solutions with a volume of 10 mL with different concentrations were prepared, and 10 mL of deionized water was used as control. Measurements were repeated multiple times to ensure consistency. All measurements were carried out at a temperature of 298K. The adsorption characteristics: surface excess ($\Gamma_{max}$), surface area per molecule ($A_{min}$), standard free energy of micellization ($\Delta G_m$) were calculated using equations (eqS1) - (eqS4) according to Refs. [52–54].

### 2.3. Solubilization

To a series of surfactant solutions excess powder of Orange OT, a hydrophobic solubilization probe, was added and the solutions were equilibrated for 48 h. After the solubilization process, samples were analyzed on Analytik Jena Specord 250 PLUS for their Orange OT content, using absorption coefficient of 17400 L $mol^{-1}cm^{-1}$ at 495 nm. Obtained plots were used for linear approximation of the segment above the critical micelle concentration (CMC) to determine solubilization capacity (moles of hydrophobic probe per moles of surfactant) as the slope of the linear approximation according to eqS5.

### 2.4. Fluorimetry

A stock solution of pyrene in ethanol was added to the aqueous surfactant samples to obtain final concentration of 0.6 μM. Samples were then analyzed in the range of 350–500 nm on Hitachi F-7100 spectrofluorimeter using 335 nm excitation wavelength. Values of the first and third pyrene fluorescence peak were compared to obtain the polarity parameter ($I_1/I_3$). The CMC was determined from the abrupt change in this polarity parameter by approximating the experimentally obtained points to the Boltzmann sigmoid equation in the Origin Pro 2021 software version 9.8.0.200 [55].

### 2.5. Liposome preparation

Lipid films were formed by aliquoting fresh pre-made stock solutions of lipids or surfactants in chloroform into an empty vessel. Total lipid concentration in all samples was 3 mM PC and 2 mM Chol. DOTAP or carbamate gemini surfactants were added the same way at molar ratios of 1/10–1/100 of the sum of PC and Chol content. The dried films were hydrated with 25 mM HEPES buffer at pH = 7.4. The amphiphilic peptide

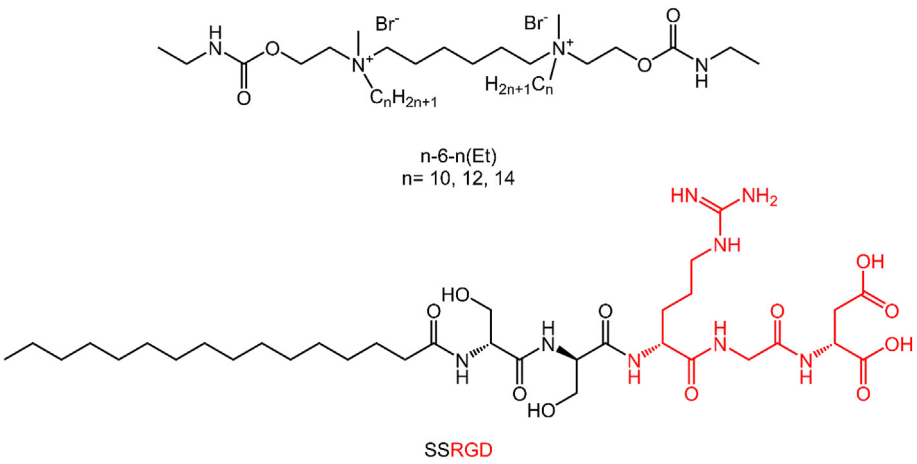


**Fig. 1.** General structural formula of the studied cationic carbamate gemini surfactants n-6-n(Et) and amphiphilic peptide SSRGD.

SSRGD was added by dissolving it in the buffer and adding it at the hydration stage, where it localized in the lipid bilayer. C6 at molar ratio of 1/150$^{th}$ of the PC and Chol sum was loaded to detect liposomes via fluorescence by adding its chloroform solution to the initial lipid film. Liposomes were prepared using thin film hydration, 5x freeze-thaw cycles, and extrusion (LiposoFast LF-50 extruder) using 100 nm porous membranes (Whatman).

### 2.6. Liposome characterization

Dynamic and electrophoretic light scattering on Zetasizer Nano device (Malvern, United Kingdom) were employed to obtain particle size and zeta potential distributions. Time of signal accumulation was 60 s for size measurements and automatically selected number of 5-s runs for zeta potential measurement (usually 11–15 runs) at a fixed scattering angle 173°. The raw correlation data were converted to hydrodynamic diameters, polydispersity indices (PdI) and zeta potentials (ZP) within Zetasizer Software (Malvern) version 7.11. Samples were diluted to 1 mM of total concentration for analysis.

Transmission electron microscopy (TEM) images were obtained at the interdisciplinary center "analytical microscopy" of Kazan Federal University, using a Hitachi HT7700 Exalens microscope, Japan. The images were acquired at an accelerating voltage of 100 kV. Samples were dispersed on 300 mesh 3 mm copper grids (Ted Pella) with continuous carbon-formvar support films.

### 2.7. Antimicrobial activity

Gram-positive bacteria *Staphylococcus aureus ATCC 209p (Sa), Bacillus cereus ATCC 8035 (Bc), Enterococcus faecalis ATCC 29212 (Ef),* Methicillin-resistant strains of *S. aureus* (*MRSA-1*) and (*MRSA-2*) were isolated from the body of patients with chronic tonsillitis and sinusitis in the bacteriological laboratory of the Republican Clinical Hospital (Kazan, Russia); *Escherichia coli ATCC 25922 (Ec), Pseudomonas aeruginosa ATCC 9027 (Pa)* and yeast *Candida albicans ATCC 10231 (Ca)* were used to evaluate the antimicrobial activity of the carbamate gemini surfactants. The bacteriostatic and fungistatic activity was studied in Muller Hinton Broth 2 (bacteria $3 \times 10^5$ cfu mL$^{-1}$) and Sabouraud dextrose broth (fungi $2 \times 10^3$ cfu mL$^{-1}$). Ciprofloxacin and ketoconazole were used as comparison. The results were recorded every 24 h for 5–14 days. Cultures were incubated with test compounds diluted in series in nutrient media at 25–37°C. The minimum inhibitory concentration (MIC) was defined as the minimum concentration of a compound that inhibits the growth of the corresponding test microorganism. The minimum bactericidal (MBC) and fungicidal (MFC) concentrations were determined as the concentrations of added compounds, at which an attempt to recultivate cells in Mueller-Hinton or Sabouraud dextrose agar for 24–48 h at 25–37°C was not successful [56]. The experiment was repeated three times.

### 2.8. Cell cultures

For the experiments, we used a tumor cell culture PC-3 - adenocarcinoma of the prostate gland from ATCC (American Type Cell Collection, USA; CRL 1435) and a healthy cell line WI-38 – VA 13 subline 2RA – human embryo lung from Institute of Cytology of Russian Academy of Sciences (Saint-Petersburg, Russia).

### 2.9. Cytotoxicity

The cytotoxic effect on cells was determined using the MTT test. Cells were seeded on a 96-well Nunc plate at a concentration of $5 \times 10^3$ cells per well in a volume of 100 μL of medium and cultured in a $CO_2$ incubator at 37°C until a monolayer was formed. Then the nutrient medium was removed and 100 μL of solutions of the tested composition in the given dilutions were added to the wells, which were prepared directly in the nutrient medium with the addition of 5% DMSO to improve solubility. After 24 h of incubation of the cells with the test compounds, the nutrient medium was removed from the plates and 100 μL of the nutrient medium without serum with MTT at a concentration of 0.5 mg mL$^{-1}$ was added and incubated in a $CO_2$ incubator for 4 h at 37°C. After incubation, the medium with MTT was removed and to dissolve the formed formazan crystals, 100 μL of DMSO was added to each well. Optical density was recorded at 540 nm on an Invitrologic microplate reader (Russia). The experiments for all compounds were repeated three times. Calculation of $IC_{50}$, the concentration of the test compound that causes suppression of cell growth by 50%, was made using the program: MLA - "Quest Graph ™ IC50 Calculator". AAT Bioquest, Inc.

### 2.10. Flow cytometry

PC-3 cells at $1 \times 10^6$ cells/well in a volume of 2 mL were added to 6-well plates and cultured in a $CO_2$ incubator at 37°C in an atmosphere containing 5% $CO_2$ until a monolayer was formed. Then the nutrient medium was taken and solutions in the nutrient medium of various concentrations of the studied compositions were added to the wells. The plates were cultured in a $CO_2$ incubator at 37°C in an atmosphere containing 5% $CO_2$ for 24 h. Coumarin 6 dye was used as a fluorescent probe. Treated cells were analyzed by flow cytometry (Guava easy Cyte, Merck, USA). The experiments were repeated three times and data was reported as mean fluorescence intensity (M.F.I.) values ± standard deviation.

### 2.11. Fluorescence microscopy

PC-3 cells at 1x10$^5$ cells/well were plated in 6-well plates with coverslips at the bottom of each well. After 24 h of incubation, samples were added to the wells and cultured for 24 h in $CO_2$- incubator. Then, after treatment with test systems, PC-3 cells were fixed and stained with DAPI (blue). The studies were carried out on a Nikon Eclipse Ci-S fluorescent microscope (Nikon, Japan) at a magnification of 400×.

### 2.12. Statistical analysis

The $IC_{50}$ was calculated using an online calculator: MLA - Quest Graph ™ IC50 Calculator. AAT Bioquest, Inc, May 11, 2022, https://www.aatbio.com/tools/ic50-calculator. Statistical analysis was performed using the Mann-Whitney test ($p < 0.05$).

## 3. Results

### 3.1. Aggregation and micellar properties

Low aggregation thresholds for the gemini surfactants are well-documented [57]. In our case, a clear trend of CMC decrease can be seen with the elongation of the surfactant tails (Fig. 2, Table 1), where each addition of two methylene groups lowers the CMC by an order of magnitude. So, the 14-carbon bearing compound 14-6-14(Et) starts to form aggregates at as low as 30 μM, while surfactant with the shortest tails 10-6-10(Et) has a comparable CMC to the classic 16-carbon cationic surfactant representatives such as cetyltrimethylammonium bromide (CTAB) in the millimolar range.

Thermodynamic parameters of aggregation can be derived from tensiometry data, such as minimal equilibrium surface area per surfactant molecule $A_{min}$, surface excess $\Gamma_{max}$, and free energy of micelle formation $\Delta G_{mic}$ (Table 2). Analysis of free energy of micelle formation dependence on surfactant tail length can be used to obtain free energy of methylene group transport from water to the hydrophobic micellar core, for which a value of −3.0 kJ/mol was obtained (Fig. S10), which is close to the literature data [14].

The solubilization plots (Figs. S11–S13) provide two important characteristics of the studied surfactants: CMC and solubilization capacities. The determined values can be found in Table 1. Since surfactants with longer tails can form micelles with larger hydrophobic cores and embed more of the hydrophobic dye, thus higher solubilization capacity is observed for 14-6-14(Et).

Pyrene fluorescence assay is a very powerful technique that allows to not only determine the micellization thresholds, but also to compare micellar micropolarity conditions for different surfactants. The CMC values are presented in Table 1, while on the plot (Fig. S14) it can be seen that 10-6-10(Et) reaches a plateau after the inflection at 1.62 units of polarity parameter ($I_1/I_3$), whereas for 14-6-14(Et) the final polarity after inflection point is lower at 1.55 units. The longer hydrophobic chains, the lower the polarity inside micelles, however it is noteworthy, that even for 14-6-14(Et) very high polarity is observed compared to traditional surfactants, where usually values of 1.3–1.4 units are recorded in the micellar region [55]. Such high micellar polarity parameter may be caused by a large polar headgroup containing two carbamate fragments surrounded with solvate shell and allowing water to penetrate to the palisade layer.

**Table 1**
CMC values of the investigated surfactants obtained by various methods and their solubilization capacity, 25 °C.

| Surfactant | CMC, M | | | $S$, $mol_{Orange\ OT}/mol_{Surfactant}$ |
|---|---|---|---|---|
| | Tensiometry | Solubilization | Fluorimetry | Solubilizing capacity |
| 10-6-10(Et) | $5.8 \bullet 10^{-3}$ | $5.7 \bullet 10^{-3}$ | $4.8 \bullet 10^{-3}$ | 0.015 |
| 12-6-12(Et) | $5 \bullet 10^{-4}$ | $5 \bullet 10^{-4}$ | $3.9 \bullet 10^{-4}$ | 0.024 |
| 14-6-14(Et) | $3 \bullet 10^{-5}$ | $4 \bullet 10^{-5}$ | $4.3 \bullet 10^{-5}$ | 0.032 |

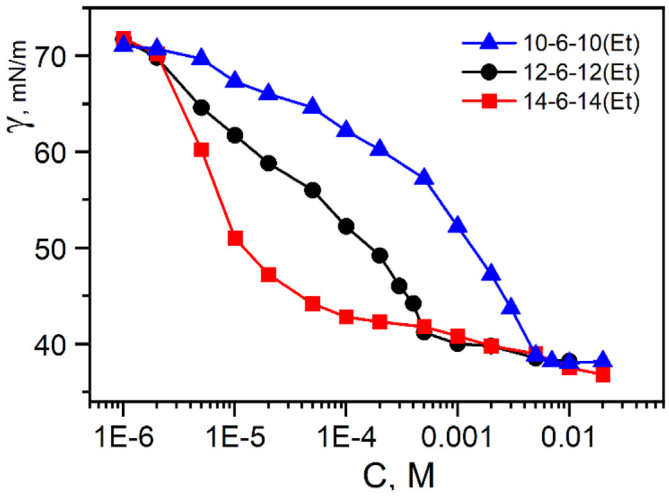


**Fig. 2.** Surface tension isotherms for the carbamate gemini surfactants, 25 °C.

**Table 2**
Adsorption parameters and free energy of micelle formation for carbamate gemini surfactants, 25 °C.

| Surfactant | $\Gamma_{max}$*10$^{10}$, mol/cm$^2$ | $A_{min}$, nm$^2$ | $\Delta G_{mic}$, kJ/mol |
|---|---|---|---|
| 10-6-10(Et) | 1.01 | 1.65 | −28.1 |
| 12-6-12(Et) | 0.78 | 2.12 | −34.2 |
| 14-6-14(Et) | 1.39 | 1.19 | −40.3 |

### 3.2. Antimicrobial activity of gemini surfactants

As a novel series, the carbamate gemini surfactants were tested for their antimicrobial activity in the framework of routine analysis along with self-aggregation, since ammonium surfactants often act as efficient antimicrobial agents. Gram-positive *S. aureus* (*Sa*), *B. cereus* (*Bc*), *E. faecalis* (*Ef*) and Gram-negative bacteria *E. coli* (*Ec*), *P. aeruginosa* (*Pa*), including methicillin-resistant strains of *S. aureus MRSA-1* (resistance to antibiotics of the fluoroquinolone and β-lactam series) and *MRSA-2* (resistance only to antibiotics of β-lactam series) were chosen as study objects. Antifungal activity was studied on *Candida albicans* (*Ca*). The minimum inhibitory concentration (MIC) values are shown in Table 3.

The carbamate gemini surfactants show strong antimicrobial activity compared to both antibiotic ciprofloxacin and antifungal agent ketoconazole, as well as traditional ammonium surfactant CTAB. MIC values of n-6-n(Et) surfactants toward Gram-positive *Sa, Bc, Ef* strains are in the near order with Ciprofloxacin, while 10-6-10(Et) and 14-6-14(Et) are considerably weaker toward gram-negative bacteria than the control antibiotic. However, while ciprofloxacin causes much less toxicity to *MRSA-1*, carbamate gemini surfactants maintain MIC values in the microgram range, being up to 250 times more toxic than ciprofloxacin. Among the surfactants 12-6-12(Et) is most toxic toward all bacteria, and 14-6-14(Et) is the least toxic.

### 3.3. Liposome cationization with DOTAP and carbamate gemini surfactants

To formulate liposomes, soybean PC and cholesterol were used as the basic lipid material in HEPES buffer conditions (pH 7.4). Cholesterol is used as an additive for liposome formulations to increase their stability

**Table 3**
*In vitro* antibacterial and antifungal activities of the gemini surfactants.

| Compounds | MIC* – minimum inhibitory concentration (μg mL$^{-1}$) | | | | | | | |
|---|---|---|---|---|---|---|---|---|
| | *Sa* | *Bc* | *Ef* | MRSA-1 | MRSA-2 | *Ec* | *Pa* | *Ca* |
| 10-6-10(Et) | 0.9 ± 0.07 | 1.9 ± 0.1 | 0.9 ± 0.07 | 0.5 ± 0.04 | 0.5 ± 0.03 | 3.9 ± 0.2 | 31.3 ± 2.6 | 62.5 ± 5.4 |
| 12-6-12(Et) | 0.5 ± 0.04 | 0.9 ± 0.07 | 0.9 ± 0.06 | 0.5 ± 0.03 | 0.5 ± 0.04 | 0.9 ± 0.07 | 3.9 ± 0.2 | 3.9 ± 0.2 |
| 14-6-14(Et) | 3.9 ± 0.2 | 3.9 ± 0.3 | 3.9 ± 0.2 | 1.9 ± 0.1 | 1.9 ± 0.1 | 15.6 ± 1.2 | 62.5 ± 5.4 | 15.6 ± 1.3 |
| Ciprofloxacin | 0.5 ± 0.03 | 0.5 ± 0.04 | 3.9 ± 0.3 | 125 ± 11 | 0.9 ± 0.07 | 0.5 ± 0.03 | 0.5 ± 0.03 | – |
| Ketoconazole | – | – | – | – | – | – | – | 3.9 ± 0.3 |
| CTAB* | 0.5 | 3.1 | – | – | – | 6.3 | 250 | 3.1 |
| MBC* – minimum bactericidal concentration (μg mL$^{-1}$) | | | | | | | | Minimum fungicidal concentration (MFC), μg mL$^{-1}$ |
| 10-6-10(Et) | 7.8 ± 0.6 | 15.6 ± 1.2 | 31.3 ± 2.3 | 0.5 ± 0.05 | 0.5 ± 0.04 | 15.6 ± 1.2 | – | 62.5 ± 5.5 |
| 12-6-12(Et) | 31.3 ± 2.5 | 15.6 ± 1.3 | 3.9 ± 0.2 | 0.5 ± 0.05 | 0.5 ± 0.03 | 7.8 ± 0.5 | – | 3.9 ± 0.2 |
| 14-6-14(Et) | 62.5 ± 5.3 | 15.6 ± 1.1 | 31.3 ± 2.5 | 1.9 ± 0.1 | 1.9 ± 0.1 | 15.6 ± 1.2 | – | 15.6 ± 1.3 |
| Ciprofloxacin | 0.5 ± 0.03 | 0.5 ± 0.04 | 3.9 ± 0.3 | 250 ± 19 | 0.9 ± 0.06 | 0.5 ± 0.03 | 0.5 ± 0.03 | – |
| Ketoconazole | – | – | – | – | – | – | – | 3.9 ± 0.3 |
| CTAB* | 50 | >500 | – | – | – | >500 | >500 | 50 |

* – Average of three values measured; ± standard deviation (SD).
* – Cetyltrimethylammonium bromide, data from Ref. [58].

and to prolong the release rate of encapsulated drug. Based on fundamental researches [59,60], we opted to use 40 mol% of cholesterol from the total amount of lipids employed in the liposome formation. The buffer conditions provide control of the ionization state of all of the groups present on top of liposomes, that better corresponds to *in vivo* conditions. This control is essential, since liposome charge can strongly affect cellular uptake.

The carbamate gemini surfactants were tested as liposome modifiers that provide a positive charge and compared to a widely used cationic lipid DOTAP (Table 4). In buffer conditions, it can be seen that addition of 1/100$^{th}$ of DOTAP is not enough to significantly shift the zeta potential of liposomes towards the positive. Only at the ratio of 1/35$^{th}$ a significant charge of +19.5 mV is achieved, and further increase of DOTAP fraction up to 1/25$^{th}$ increases the potential to +26 mV. However, DOTAP is known to cause toxicity and a smaller fraction of it is preferrable [27].

To evaluate cellular uptake, liposomes were doped with 1/150$^{th}$ of fluorescent probe coumarin 6 (C6), a hydrophobic compound that is expected to localize in the liposome bilayers, which has been previously used for uptake and localization analysis [61–64], DLS data of C6 liposomes is shown on Table 5.

Considering cytotoxicity data, the surfactant 14-6-14(Et) was chosen as an optimal compound for the following work. Coumarin 6 addition to the liposomes caused a significant drop of zeta potential towards negatives, lowering plain phosphatidylcholine-based liposomes to −27 mV of zeta potential. At this point, addition of 1/50$^{th}$ of DOTAP was not enough to cationize the liposomes and the resulting potential was −4 mV. The molar DOTAP ratio of 1/25$^{th}$ results in a +20 mV, which is 6 mV lower than that of the liposomes without C6. Encapsulation of C6, however, did not significantly alter the zeta potential of liposomes modified with 14-6-14(Et) which confirms that in buffer conditions DOTAP has a weak ability to induce a positive charge on the liposomes, and carbamate gemini surfactants are more fitting for this purpose.

TEM images show a dense population of vesicular aggregates with a clearly distinguishable shells 4–6 nm in thickness which correspond well to a lipid bilayer thickness (Fig. 3). On the DOTAP-doped sample, mostly, deformed large aggregates of 200–400 nm in diameter are seen, which are most likely products of fusion of smaller vesicles. Smaller liposomes can be also distinguished consisting of one or two, rarely three lamellae with average diameters of 70–150 nm. On the 14-6-14(Et) liposome sample more of the aggregates appear to be of original shape, with more than half of them being elongated round vesicles with diameters ranging from 50 to 200 nm. Significantly fewer large vesicles can be observed on this sample, indicating a smaller degree of intervesicular fusion. Small proportion of the population consists of multi-layered vesicles having 2–3 lamellae. In less crowded areas of the sample mostly singular spherical aggregates are observed (Fig. S15).

### 3.4. *In vitro* liposome performance: toxicity and cell association enhancement

Cytotoxicity of surfactant modified liposomes increases with the increase of surfactant incorporation fraction (Fig. 4). The $IC_{50}$ values in the range of 0.19–0.39 mM correspond to surfactant concentrations below the CMC, so the cytotoxic effect is mainly attributed to the monomeric and liposome-incorporated form of the gemini.

For the comparison of cellular uptake, a commonly used peptide motif

**Table 4**
DLS parameters of liposomes obtained with different cationic modifiers at various molar ratios, HEPES pH 7.4, 25 °C. Data are represented as mean standard ± deviation (n = 3).

| Additive type | Molar ratio Additive/lipid | $D_H$, nm | PdI | ZP, mV |
|---|---|---|---|---|
| Control | – | 118 ± 1 | 0.078 | −6.9 ± 0.5 |
| DOTAP | 1/100 | 124 ± 2 | 0.138 | −1.2 ± 1.2 |
| DOTAP | 1/50 | 109 ± 1 | 0.090 | +11.1 ± 0.3 |
| DOTAP | 1/35 | 104 ± 1 | 0.096 | +19.5 ± 0.5 |
| DOTAP | 1/25 | 97 ± 1 | 0.093 | +26.2 ± 1.6 |
| 10-6-10(Et) | 1/25 | 111 ± 1 | 0.075 | +18.0 ± 1.4 |
| 12-6-12(Et) | 1/25 | 117 ± 1 | 0.086 | +40.7 ± 1.5 |
| 14-6-14(Et) | 1/25 | 105 ± 2 | 0.090 | +48.3 ± 1.8 |
| SSRGD | 1/100 | 115 ± 2 | 0.094 | −34.7 ± 1.4 |
| SSRGD | 1/50 | 102 ± 2 | 0.106 | −31.4 ± 1.8 |
| SSRGD | 1/35 | 107 ± 2 | 0.090 | −33.3 ± 0.5 |
| SSRGD | 1/25 | 100 ± 1.5 | 0.081 | −39.6 ± 1.0 |

**Table 5**
The effect of coumarin 6 on DLS parameters of liposomes obtained with different cationic modifiers at various molar ratios, HEPES pH 7.4, 25 °C. Data are represented as mean standard ± deviation (n = 3).

| Additive type | Molar ratio Additive/lipid | $D_H$, nm | PdI | ZP, mV |
|---|---|---|---|---|
| Control C6 | – | 130 ± 1 | 0.081 | −26.6 ± 1.2 |
| DOTAP C6 | 1/50 | 116 ± 2 | 0.083 | −5.0 ± 0.2 |
| DOTAP C6 | 1/35 | 110 ± 3 | 0.066 | +7.7 ± 0.4 |
| DOTAP C6 | 1/25 | 101 ± 1 | 0.069 | +18.9 ± 0.9 |
| DOTAP C6 | 1/12.5 | 101 ± 2 | 0.143 | +30.5 ± 0.7 |
| 14-6-14(Et) C6 | 1/50 | 109 ± 3 | 0.103 | +23.8 ± 1.0 |
| 14-6-14(Et) C6 | 1/35 | 102 ± 5 | 0.078 | +36.6 ± 1.7 |
| 14-6-14(Et) C6 | 1/25 | 97 ± 4 | 0.149 | +45.6 ± 1.8 |
| SSRGD C6 | 1/25 | 120 ± 1 | 0.166 | −23.8 ± 0.9 |
| SSRGD DOTAP C6 | 1/25 + 1/35 | 117 ± 2 | 0.122 | +12.6 ± 0.3 |
| SSRGD 14-6-14(Et) C6 | 1/25 + 1/35 | 123 ± 1 | 0.140 | +17.3 ± 1.5 |

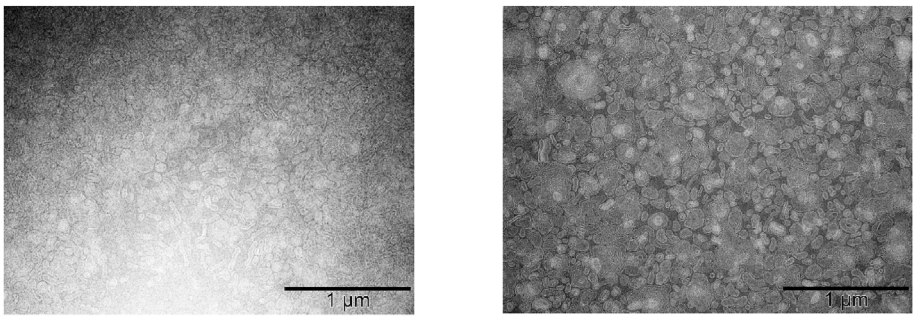


**Fig. 3.** TEM images of liposomes modified with DOTAP and 14-6-14(Et).

that enhances cellular uptake, RGD [65], in its amphiphilic form (SSRGD) was also incorporated into the liposome bilayers, and no effect on cytotoxicity toward PC-3 was observed with varied SSRGD concentration, which illustrates its complete biocompatibility in the studied concentration range (Fig. S16).

Formulation of liposomes that are highly capable to infiltrate cells would require two important aspects: positive charge and RGD modification. In order to compare individual effects of different modifiers (cations or SSRGD) on cytotoxicity, a comparative assay on PC-3 and WI-38 cells was conducted. Firstly, it is noteworthy that all prepared compositions loaded with C6 showed much higher cytotoxicity toward PC-3 cancer cells compared to healthy WI-38 cells (Fig. 5). The most toxic toward both cells were cationic SSRGD-modified compositions including DOTAP or 14-6-14(Et), which may be explained by the fact that cationic lipids or the surfactant are cytotoxic on their own, and RGD being a tissue uptake inductor amplifies the toxic effect by introducing more liposome particles into the cells. Liposomes, which were cationized using DOTAP, in both cell lines show more toxicity, where the cationic carbamate gemini surfactant stands out as a more biocompatible positive charge inductor. Moreover, the zeta potential of 14-6-14(Et) modified liposomes is much higher than that of DOTAP modified liposomes at the same ratios, which is beneficial in terms of cellular uptake. Flow cytometry data show increased association of cationic liposomes with cells as evident by mean fluorescence intensity of coumarin 6 associated with liposomes (Fig. 6).

In Fig. 7, it can be clearly seen that 14-6-14(Et) modified liposomes show the highest association among the non-RGD liposome group and among the RGD-modified group. The combination of RGD and cationic charge is strongly distinct from individual modulators such as DOTAP or RGD peptide on their own. Among cationic RGD-modified liposomes, 14-6-14(Et) liposomes are more readily absorbed probably due to their stronger positive charge.

### 3.5. *Fluorescence microscopy and performance with doxorubicin*

Fluorescence microscopy allows to simultaneously trace cell nuclei (DAPI, blue), liposomes (coumarin 6, green), and DOX (red) in PC-3 cell line (Fig. 8). The studied samples included DAPI individually and all dyes in free form as control (Fig. S17), as well as unmodified PC Chol liposomes, 14-6-14(Et) liposomes and 14-6-14(Et) + SSRGD liposomes (Fig. 8). Throughout the experiment intense red fluorescence was observed in cell nuclei and cytoplasm indicating successful DOX delivery into the cells. Green fluorescence of C6, associated with liposome bilayers, localized noticeably in the membrane region of cells in case of neutral liposomes in the first 6 h of incubation. For cationized and RGD modified liposomes a less pronounced membrane localization is observed, indicating that liposomes are entering the cytoplasm more rapidly. After 24 h in PC-Chol samples C6 fluorescence was more evenly spread throughout the cells indicating internalization or diffusion of C6 into the cytoplasm. By this time, samples with 14-6-14(Et) and dual-modified liposomes with SSRGD resulted in noticeable cell deformation indicating nuclei fragmentation into apoptotic bodies.

MTT assay of DOX action toward PC-3 and WI-38 cells (Fig. 9) revealed selectivity toward the prostate cancer cell line which was maximal for the liposomes modified with 14-6-14(Et). Liposomes did not significantly alter $IC_{50}$ values of DOX in case of PC-3 cells but produced less toxicity when incubated with WI-38 cells. Modification with the cationic surfactant 14-6-14(Et) decreases cytotoxicity of DOX-carrying liposomes toward healthy WI-38 cells.

## 4. Discussion

Among the broad spectrum of carbamate gemini surfactants with different tail lengths, we can observe that there is a non-linear dependence of liposome zeta potential on the surfactant tail length (Table 4).

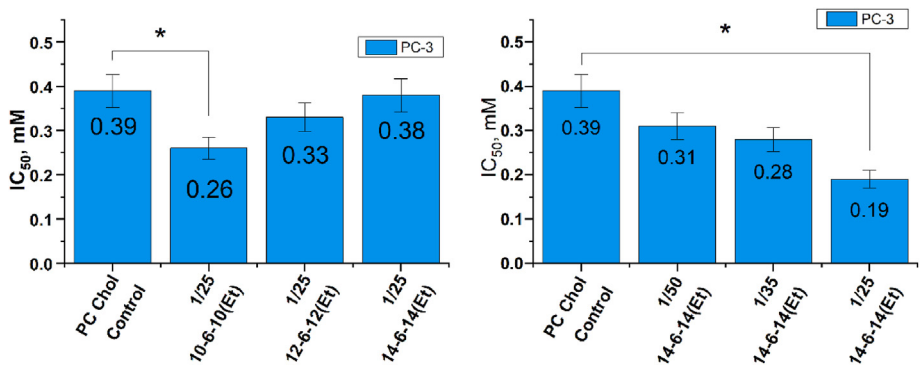


**Fig. 4.** Cytotoxicity of liposomes, modified with different tail lengths carbamate gemini surfactants on PC-3 cells. Effect of tetradecyl carbamate gemini surfactant 14-6-14(Et) on cytotoxicity toward PC-3 cells, with the lipid/surfactant molar ratio varied. *$p < 0.05$.

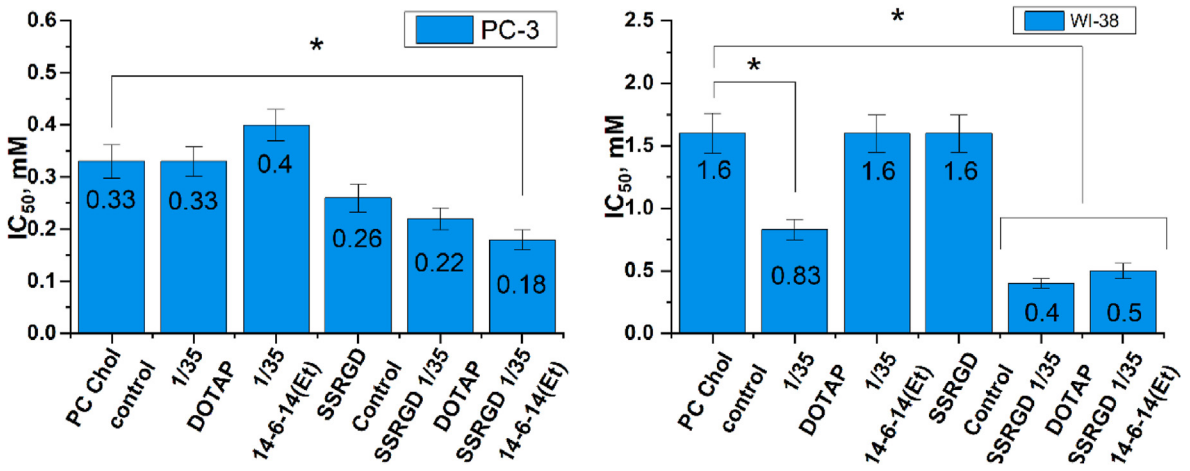


**Fig. 5.** Cytotoxicity of cationic liposomes obtained via modification with DOTAP or 14-6-14(Et) with and without the addition of RGD toward PC-3 and WI-38 cells. *p < 0.05.

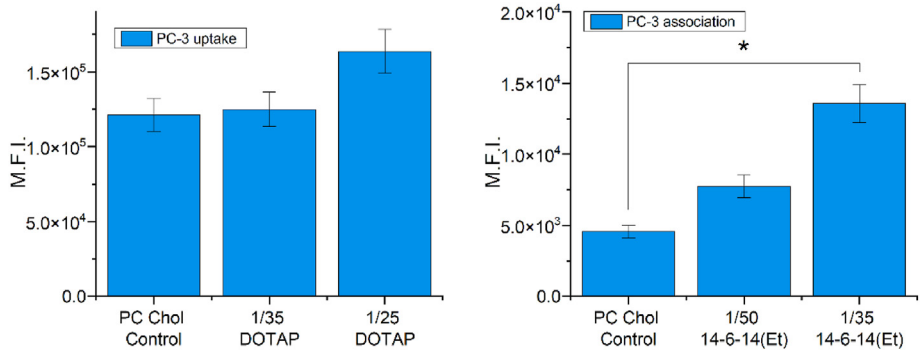


**Fig. 6.** Comparison of DOTAP and 14-6-14(Et) for cationic liposome modification and their effect on uptake by PC-3 cells. *p < 0.05.

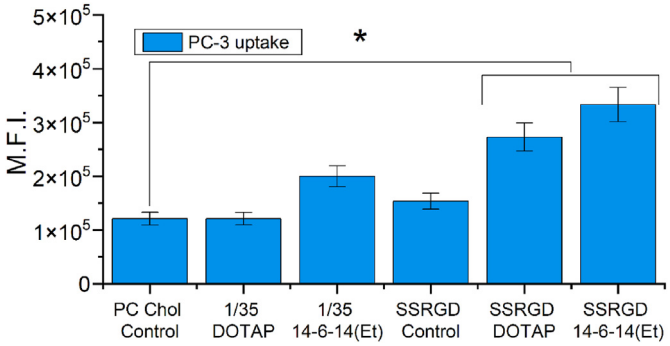


**Fig. 7.** Comparison between effects of cationic charge and SSRGD adhesive effects on association of modified liposomes with PC-3 cells. *p < 0.05.

The surfactant with shortest tails, 10-6-10(Et) provides the lowest charge of +18 mV compared to other surfactants. This may be caused by a deeper insertion of the headgroups into the lipid bilayer and masking of the cationic ammonium groups by phosphates in the vicinity. Increase of the tail length from 12 to 14 carbon atoms shows a small degree of potential increase, which may be explained by the same effect of the depth where the surfactant resides; shorter tailed ones residing a bit deeper, while head groups of higher homologues localize close to periphery, thus providing more bare charged groups on the surface. Also, similar results have been reported for lower homologs of cationic surfactants [66,67]. It is clear that at the ratio of $1/25^{th}$, most carbamate gemini surfactants provide almost twice as much zeta potential as DOTAP, which proves their efficiency as liposome charge modulators. This must be caused by the fact that a gemini surfactants provide twice as many positively charged groups per molecules than DOTAP; however, the degree of counterion binding may vary between the DOTAP ammonium group, and the first and second ammonium groups on the carbamate gemini surfactants, hence no simple correlation between the number of charged groups and zeta potential is to be expected. This is evident when comparing liposomes with the same amounts of cations, for example, the composition with $1/12.5^{th}$ of DOTAP and liposomes with $1/25^{th}$ of 14-6-14(Et). Although the amount of added cationic groups is the same in both cases, the latter have a 35% higher zeta potential than the former, instead of 2x difference.

The vesicles in the images appear very deformed: DOTAP liposomes appear to be more irregular in shape, having more curvature and showing more irregularity, than liposomes modified with 14-6-14(Et). Strong deviations from spherical shape have been observed in case of liposomes modified with polyglicidol due to strong interactions of polymer chains leading to the decrease of bilayer curvature [68], due to doxorubicin loading [69], for polymersomes [70], or caused by specific lipid shapes [71]. However, in case of PC-Chol liposomes modified with DOTAP or 14-6-14(Et) at small molar ratios (≤1/25) neither of these effects is significantly present. Most likely, the deformation observed here is caused by dense packing of the particles, where they push into each other causing deformation and fusion. In this regard, it is reasonable to expect 14-6-14(Et) liposomes to resist deformation and fusion better due to higher zeta potential, and stronger repulsion. Moreover, some discussion about the effect of gemini surfactants upon lipid bilayer has been published [72], and they are known to integrate well into the bilayer [35]. In our case, two carbamate domains at every surfactant molecule, that are

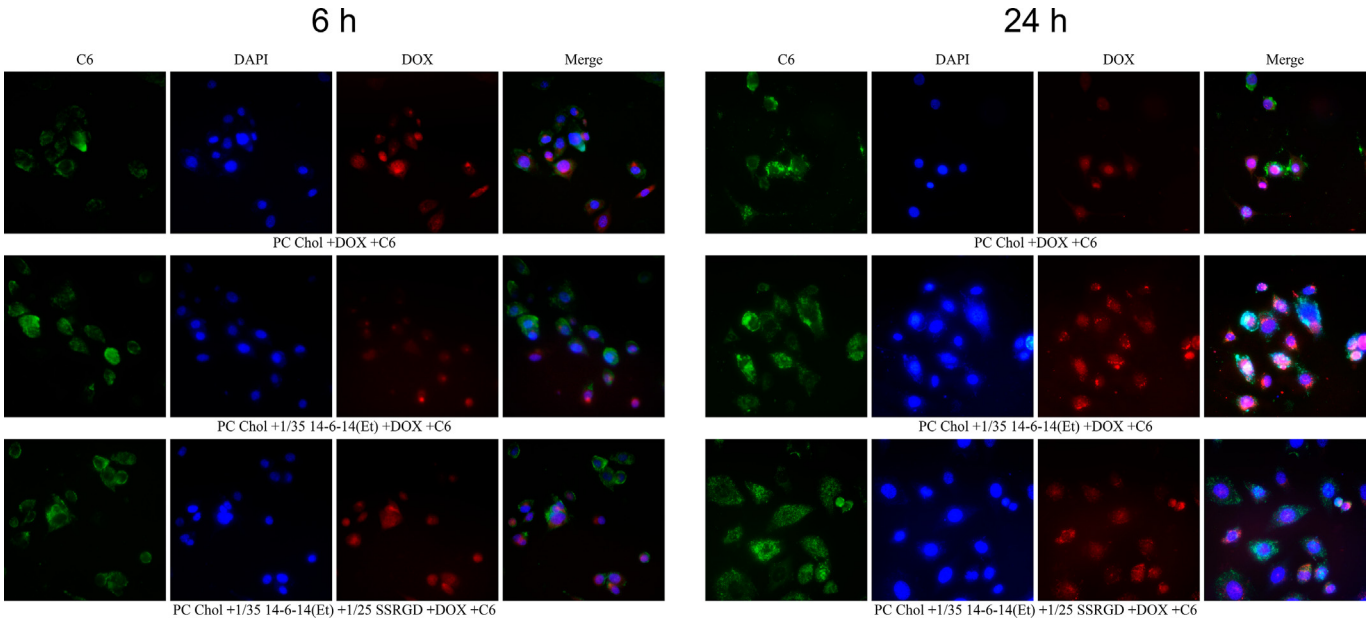


**Fig. 8.** Fluorescence microscopy of liposomes loaded with DOX and dyed with coumarin 6 in PC-3 cells stained by DAPI. 6 h incubation (left) and 24 h incubation (right). Blue channel: DAPI, DNA-intercalating dye. Red channel: DOX, DNA-intercalating drug that was administered to cells in free or liposomal form. Green channel: C6, a hydrophobic dye incorporated into liposome bilayers.

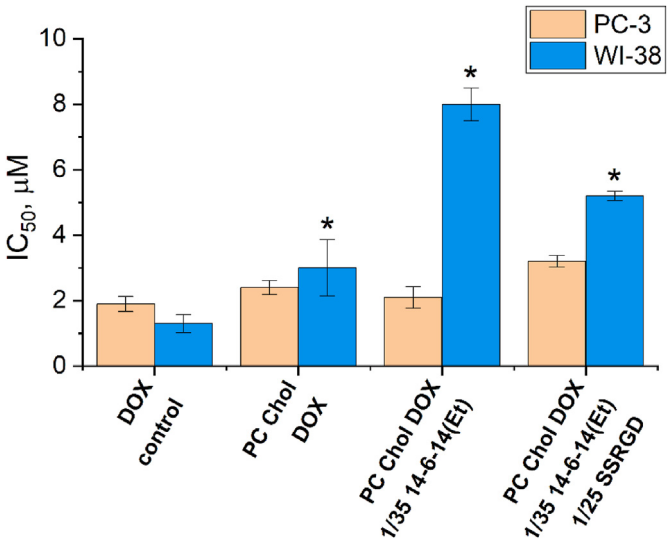


**Fig. 9.** Cytotoxicity of DOX toward PC-3 and WI-38 cells in the free form or encapsulated in plain and modified with 14-6-14(Et) and SSRGD liposomes. *p < 0.01 compared to free DOX.

most likely spread widely across the top of the bilayer plane, provide multiple sites for intermolecular interactions such as van der Waals or hydrogen interactions, and may provide additional sturdiness to the bilayers.

Usually, Gram-negative bacteria are more resistant than Gram-positive bacteria to cationic surfactants, which is associated with the structure of their membrane. This was confirmed in a number of studied compounds. It is known that antibacterial activity is highly dependent on the length of the alkyl chain, and that there is an optimal chain length for maximum antibacterial activity [73–75]. This is generally rationalized in terms of the so-called cut-off effect [76]. In our case, compound 12-6-12(Et) turned out to be the most active in the homologous series against *S. aureus:* MIC values (0.5 μg $mL^{-1}$) were comparable to those of the reference drug ciprofloxacin. This can be explained, on the one hand, by the fact that most cell wall phospholipids consist of 12 carbon atoms, and amphiphiles with dodecyl tails are closest to them in terms of physical and chemical properties and require minimal energy for incorporation [74]. On the other hand, dodecyl surfactants, compared with higher homologues, have optimal solubility for the manifestation of antibacterial activity [75].

A combination of the electrostatic and specific protein interaction adhesive effects by using a cationic liposome modified with SSRGD can be very promising. The choice of the 16-carbon hydrophobic chain is explained by its high affinity to the liposome membrane, such derivative is expected to strongly take root in the bilayer compared to lower homologues [77]. The di-serine bridge between the hydrophobic anchor of the peptide and the RGD sequence is necessary to interact with the polar palisade layer of the bilayer, where the lipid headgroups containing ester and phosphate groups are present to form multiple hydrogen interactions with. Also, serine hydrophilicity ensures that the peptide is not likely to be deeply dragged into the hydrophobic bilayer core, which allows for the RGD part to stick out. Cationic component exploits Coulomb interactions and the peptide enables specific binding to PC-3 membrane integrins, as was shown for a similar RGD peptide previously [27]. These are separate effects which should be combined to achieve best nanocarrier performance.

From the standpoint of the interdisciplinary approach to nanomedicine, zeta potential is a physicochemical nanocarrier characteristic which can affect *in vitro* or *in vivo* performance such as cellular uptake or association. It is logical to expect a relationship between these values, since it is known that cell membranes possess negative potential and an electrostatic attraction plays a role in nanoparticle adsorption to the membrane, which leads to uptake. In our case, both cationic components do increase uptake, however the carbamate gemini surfactants produce a much stronger effect than DOTAP, which is probably because each surfactant molecule provides two nitrogen cations and a higher zeta potential overall (Fig. 6). It is clear from flow cytometry data, that increase of the amount of cationic surfactant in liposomes leads to proportionally increased association with PC-3 cells. Similar study comparing flow cytometry results of association of liposomes with various DOTAP content with PC-3 cells concluded that charge is not as significant as PEGylation, and no simple relation between DOTAP fraction or zeta potential and uptake was observed [28]. The inconsistence may be

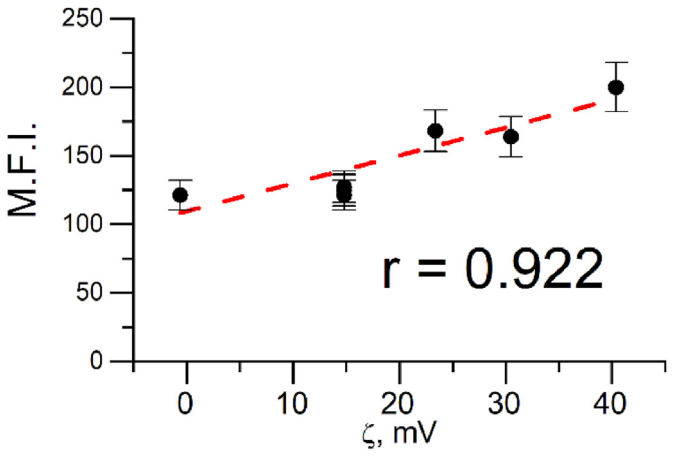


**Fig. 10.** Correlation between cellular association and liposome zeta potential.

explained by the fact that different cationizing additives and very different molar fractions were used.

Moreover, if flow cytometry data is plotted in relation to the liposome zeta potential, the Pearson's correlation is found to be 0.922 (Fig. 10) which indicates a strong connection between liposome charge and association with cells. Zeta potential and number of cationic lipids per 100 molecules in liposomes have already been correlated to *in vitro* performance. Münter and co-authors examined how these two parameters affected specificity of nanocarriers toward monocytes in human blood, but found no correlation [78].

Data obtained in this work displays the important role of zeta potential of nanoparticles in *in vitro* interactions with negatively charged biological membranes. With more data it could be possible to establish whether the relationship between zeta potential and cellular association is linear or otherwise. Nevertheless, the zeta potential is a characteristic that should be quantitatively considered in relation to nanocarrier *in vitro* performance. It is logical, since zeta-potential essentially describes how strongly a particle responds to Coulomb forces, and in case of non-specific adsorption of nanoparticles to cellular membranes, Coulomb force is what drives it.

## 5. Conclusions

The newly synthesized carbamate series of gemini surfactants displayed similar aggregation thresholds and parameters compared with other ammonium gemini surfactants. Within the framework of non-covalent approach for modifying the nanocarriers, it was demonstrated that the attractive point of these surfactants is the ability to induce a significant positive charge in liposomes, that can be used to modulate cellular uptake of the liposomes. Not only these surfactants are able to provide the same cationization to the liposomes, as DOTAP at lower cytotoxicity levels, but they also show stronger ability to increase cellular uptake of liposomes by PC-3 cancer cells (35% of cellular uptake increase by DOTAP and 190% increase by 14-6-14(Et)). The nature of uptake of cationic particles is non-specific, and it can be combined with functions that increase uptake by specific interactions for best efficacy and targeting action. Such combinations as cationic gemini surfactants and RGD functionalization are promising for further research in chemotherapy. Moreover, an evident correlation is shown between liposome zeta potential and uptake of liposomes by PC-3 cancer cells, which links a physicochemical liposome characteristic to its *in vitro* performance. Hopefully, similar results can be obtained with other cell cultures that exhibit strong negative membrane potentials. At the same time, the surfactants comply to biodegradability requirement and act as efficient tools for liposome cationization, which is a foundation for further research of such drug delivery systems for the treatment of prostate cancer.

## Declaration of competing interest

The authors declare that they have no known competing financial interests or personal relationships that could have appeared to influence the work reported in this paper.

## Acknowledgment

This work was financially supported by Russian Science Foundation (project N№ 19-73-30012).

The authors gratefully acknowledge the CSF-SAC FRC KSC RAS for providing necessary facilities to carry out this work.

## Appendix A. Supplementary data

Supplementary data to this article can be found online at https://doi.org/10.1016/j.smaim.2022.09.001.

## References

[1] M.P. Mast, H. Modh, C. Champanhac, J.W. Wang, G. Storm, J. Krämer, V. Mailänder, G. Pastorin, M.G. Wacker, Nanomedicine at the crossroads – a quick guide for IVIVC, Adv. Drug Deliv. Rev. 179 (2021), 113829, https://doi.org/10.1016/j.addr.2021.113829.

[2] M. Rizwanullah, M.Z. Ahmad, A. Garg, J. Ahmad, Advancement in design of nanostructured lipid carriers for cancer targeting and theranostic application, Biochim. Biophys. Acta - Gen. Subj. 1865 (2021), 129936, https://doi.org/10.1016/j.bbagen.2021.129936.

[3] E. Beltrán-Gracia, A. López-Camacho, I. Higuera-Ciapara, J.B. Velázquez-Fernández, A.A. Vallejo-Cardona, Nanomedicine Review: Clinical Developments in Liposomal Applications, vol. 10, Springer Vienna, 2019, ISBN 1264501900.

[4] R. Suzuki, D. Omata, Y. Oda, J. Unga, Y. Negishi, K. Maruyama, Nanomaterials in pharmacology, in: Z.-R. Lu, S. Sakuma (Eds.), Methods in Pharmacology and Toxicology, Springer, New York, NY, 2016, ISBN 978-1-4939-3120-0. New York.

[5] S. Behzadi, V. Serpooshan, W. Tao, M.A. Hamaly, M.Y. Alkawareek, E.C. Dreaden, D. Brown, A.M. Alkilany, O.C. Farokhzad, M. Mahmoudi, Cellular uptake of nanoparticles: journey inside the cell, Chem. Soc. Rev. 46 (2017) 4218–4244, https://doi.org/10.1039/c6cs00636a.

[6] S. Khan, S. Mansoor, Z. Rafi, B. Kumari, A. Shoaib, M. Saeed, S. Alshehri, M.M. Ghoneim, M. Rahamathulla, U. Hani, et al., A review on nanotechnology: properties, applications, and mechanistic insights of cellular uptake mechanisms, J. Mol. Liq. 348 (2022), 118008, https://doi.org/10.1016/j.molliq.2021.118008.

[7] Z. Zhao, A. Ukidve, V. Krishnan, S. Mitragotri, Effect of physicochemical and surface properties on in vivo fate of drug nanocarriers, Adv. Drug Deliv. Rev. 143 (2019) 3–21, https://doi.org/10.1016/j.addr.2019.01.002.

[8] E. Fröhlich, The role of surface charge in cellular uptake and cytotoxicity of medical nanoparticles, Int. J. Nanomedicine 7 (2012) 5577–5591, https://doi.org/10.2147/IJN.S36111.

[9] R. Vanbever, C. Loira-Pastoriza, N. Dauguet, C. Hérin, S. Ibouraadaten, K. Vanvarenberg, B. Ucakar, D. Tyteca, F. Huaux, Cationic nanoliposomes are efficiently taken up by alveolar macrophages but have little access to dendritic cells and interstitial macrophages in the normal and CpG-stimulated lungs, Mol. Pharm. 16 (2019) 2048–2059, https://doi.org/10.1021/acs.molpharmaceut.9b00033.

[10] C.R. Miller, B. Bondurant, S.D. McLean, K.A. McGovern, D.F. O'Brien, Liposome-cell interactions in vitro: effect of liposome surface charge on the binding and endocytosis of conventional and sterically stabilized liposomes, Biochemistry 37 (1998) 12875–12883, https://doi.org/10.1021/bi980096y.

[11] Y. Xia, J. Tian, X. Chen, Effect of surface properties on liposomal siRNA delivery, Biomaterials 79 (2016) 56–68, https://doi.org/10.1016/j.biomaterials.2015.11.056.

[12] M. Hirose, T. Ueno, H. Nagumo, Y. Sato, K. Sakai-Kato, Enhancing the endocytosis of phosphatidylserine-containing liposomes through tim4 by modulation of membrane fluidity, Mol. Pharm. 19 (2022) 91–99, https://doi.org/10.1021/acs.molpharmaceut.1c00645.

[13] J.H. Kang, W.Y. Jang, Y.T. Ko, The effect of surface charges on the cellular uptake of liposomes investigated by live cell imaging, Pharm. Res. 34 (2017) 704–717, https://doi.org/10.1007/s11095-017-2097-3.

[14] C. Bombelli, A. Stringaro, S. Borocci, G. Bozzuto, M. Colone, L. Giansanti, R. Sgambato, L. Toccaceli, G. Mancini, A. Molinari, Efficiency of liposomes in the delivery of a photosensitizer controlled by the stereochemistry of a gemini surfactant component, Mol. Pharm. 7 (2010) 130–137, https://doi.org/10.1021/mp900173v.

[15] S. Borocci, G. Bozzuto, C. Bombelli, F. Ceccacci, G. Formisano, A. Stringaro, A. Molinari, G. Mancini, How stereochemistry of lipid components can affect lipid organization and the route of liposome internalization into cells, Nanoscale 13 (2021) 11976–11993, https://doi.org/10.1039/d1nr02175c.

[16] K. Zouliati, P. Stavropoulou, M. Chountoulesi, N. Naziris, S. Demisli, E. Mitsou, V. Papadimitriou, M. Chatzidaki, A. Xenakis, C. Demetzos, Development and evaluation of liposomal nanoparticles incorporating dimethoxycurcumin. In vitro

toxicity and permeability studies, Colloids Surfaces A Physicochem. Eng. Asp. 648 (2022), 129223, https://doi.org/10.1016/j.colsurfa.2022.129223.
[17] F. Hervé, N. Ghinea, J.M. Scherrmann, CNS delivery via adsorptive transcytosis, AAPS J 10 (2008) 455–472, https://doi.org/10.1208/s12248-008-9055-2.
[18] G. Sharma, A.R. Sharma, S.S. Lee, M. Bhattacharya, J.S. Nam, C. Chakraborty, Advances in nanocarriers enabled brain targeted drug delivery across blood brain barrier, Int. J. Pharm. 559 (2019) 360–372, https://doi.org/10.1016/j.ijpharm.2019.01.056.
[19] S. Ghosh, R. Lalani, V. Patel, S. Bhowmick, A. Misra, Surface engineered liposomal delivery of therapeutics across the blood brain barrier: recent advances, challenges and opportunities, Expert Opin. Drug Deliv. (2019), https://doi.org/10.1080/17425247.2019.1676721, 0, 1.
[20] N.S. Hinge, H. Kathuria, M.M. Pandey, Engineering of structural and functional properties of nanotherapeutics and nanodiagnostics for intranasal brain targeting in Alzheimer's, Appl. Mater. Today 26 (2022), 101303, https://doi.org/10.1016/j.apmt.2021.101303.
[21] X. Yan, G.L. Scherphof, J.A.A.M. Kamps, Liposome opsonization, J. Liposome Res. 15 (2005) 109–139, https://doi.org/10.1081/LPR-64971.
[22] N. Onishchenko, D. Tretiakova, E. Vodovozova, Spotlight on the protein corona of liposomes, Acta Biomater (2021), https://doi.org/10.1016/j.actbio.2021.07.074.
[23] B. Sheikholeslami, N.W. Lam, K. Dua, M. Haghi, Exploring the impact of physicochemical properties of liposomal formulations on their in vivo fate, Life Sci 300 (2022), 120574, https://doi.org/10.1016/j.lfs.2022.120574.
[24] C. Thongbamrer, W. Roobsoong, J. Sattabongkot, P. Opanasopit, B. Yingyongnarongkul, Serum compatible spermine-based cationic lipids with nonidentical hydrocarbon tails mediate high transfection efficiency, ChemBioChem 23 (2022), https://doi.org/10.1002/cbic.202100672.
[25] Y. Zhen, K.K. Ewert, W.S. Fisher, V.M. Steffes, Y. Li, C.R. Safinya, Paclitaxel loading in cationic liposome vectors is enhanced by replacement of oleoyl with linoleoyl tails with distinct lipid shapes, Sci. Rep. 11 (2021) 1–14, https://doi.org/10.1038/s41598-021-86484-9.
[26] C.X. Du, T. Bin Zhang, S.L. Dong, L. Han, X.J. Liang, L.H. Li, Y. Wei, A magnetic gene delivery nanosystem based on cationic liposomes, J. Mater. Sci. 51 (2016) 8461–8470, https://doi.org/10.1007/s10853-016-0106-2.
[27] M. Zoughaib, R.V. Pavlov, G.A. Gaynanova, R. Garifullin, V.G. Evtugyn, T.I. Abdullin, Amphiphilic RGD and GHK peptides synergistically enhance liposomal delivery into cancer and endothelial cells, Mater. Adv. 2 (2021) 7715–7730, https://doi.org/10.1039/D1MA00498K.
[28] V.M. Steffes, Z. Zhang, S. Macdonald, J. Crowe, K.K. Ewert, B. Carragher, C.S. Potter, C.R. Safinya, PEGylation of paclitaxel-loaded cationic liposomes drives steric stabilization of bicelles and vesicles thereby enhancing delivery and cytotoxicity to human cancer cells, ACS Appl. Mater. Interfaces (2020), https://doi.org/10.1021/acsami.9b16150.
[29] C. Bode, L. Trojan, C. Weiss, B. Kraenzlin, U. Michaelis, M. Teifel, P. Alken, M. Stephan Michel, Paclitaxel encapsulated in cationic liposomes: a new option for neovascular targeting for the treatment of prostate cancer, Oncol. Rep. 22 (2009) 321–326, https://doi.org/10.3892/or_00000440.
[30] E.A. Ho, E. Ramsay, M. Ginj, M. Anantha, I. Bregman, J. Sy, J. Woo, M. Osooly-Talesh, D.T. Yapp, M.B. Bally, Characterization of cationic liposome formulations designed to exhibit extended plasma residence times and tumor vasculature targeting properties, J. Pharm. Sci. 99 (2010) 2839–2853, https://doi.org/10.1002/jps.22043.
[31] A. Stachurska, J. Elbanowski, H.M. Kowalczyńska, Role of α5β1 and αvβ3 integrins in relation to adhesion and spreading dynamics of prostate cancer cells interacting with fibronectin under in vitro conditions, Cell Biol. Int. 36 (2012) 883–892, https://doi.org/10.1042/cbi20110522.
[32] S. Naik, D. Patel, K. Chuttani, A.K. Mishra, A. Misra, In vitro mechanistic study of cell death and in vivo performance evaluation of RGD grafted PEGylated docetaxel liposomes in breast cancer, Nanomedicine Nanotechnology, Biol. Med. 8 (2012) 951–962, https://doi.org/10.1016/j.nano.2011.11.008.
[33] Z. Liu, F. Wang, X. Chen, Integrin targeted delivery of radiotherapeutics, Theranostics 1 (2011) 201–210, https://doi.org/10.7150/thno/v01p0201.
[34] A.J. Kirby, P. Camilleri, J.B.F.N. Engberts, M.C. Feiters, R.J.M. Nolte, O. Söderman, M. Bergsma, P.C. Bell, M.L. Fielden, C.L. García Rodríguez, et al., Gemini surfactants: new synthetic vectors for gene transfection, Angew. Chemie Int. Ed. 42 (2003) 1448–1457, https://doi.org/10.1002/anie.200201597.
[35] D.R. Gabdrakhmanov, E.A. Vasilieva, M.A. Voronin, D.A. Kuznetsova, F.G. Valeeva, A.B. Mirgorodskaya, S.S. Lukashenko, V.M. Zakharov, A.R. Mukhitov, D.A. Faizullin, et al., Soft nanocontainers based on hydroxyethylated geminis: role of spacer in self-assembling, solubilization, and complexation with oligonucleotide, J. Phys. Chem. C 124 (2020) 2178–2192, https://doi.org/10.1021/acs.jpcc.9b10079.
[36] L. Zhou, J. Yue, Y. Fan, Y. Wang, Self-assembly and chiral recognition of chiral cationic gemini surfactants, Langmuir 34 (2018) 12924–12933, https://doi.org/10.1021/acs.langmuir.8b02599.
[37] W. Jiao, Z. Wang, T. Liu, X. Li, J. Dong, pH and light dual stimuli-responsive wormlike micelles with a novel Gemini surfactant, Colloids Surfaces A Physicochem. Eng. Asp. 618 (2021), 126505, https://doi.org/10.1016/j.colsurfa.2021.126505.
[38] Y. Yao, Y. Fu, L. Zhang, L. Xuan, C. Qin, Synthesis, properties, and applications of an anionic–nonionic gemini surfactant for highly efficient remediation of perchloroethylene-contaminated aquifers, J. Clean. Prod. 333 (2021), 130143, https://doi.org/10.1016/j.jclepro.2021.130143.
[39] M. Sayem Alam, A. Mohammed Siddiq, M. Ali, The micellization studies of cationic gemini surfactant, hexanediyl-1,6-bis(dimethylcetylammonium bromide solutions by conductometric, tensiometric, dye solubilisation, FTIR and 1H NMR: the influence of adenosine and temperature, J. Mol. Liq. 349 (2022), 118386, https://doi.org/10.1016/j.molliq.2021.118386.
[40] C. Gan, R. Cheng, K. Cai, X. Wang, C. Xie, T. Xu, C. Yuan, Interaction of calf thymus DNA and glucose-based gemini cationic surfactants with different spacer length: a spectroscopy and DLS study, Spectrochim. Acta - Part A Mol. Biomol. Spectrosc. 267 (2022), 120606, https://doi.org/10.1016/j.saa.2021.120606.
[41] R.A. Rahimov, G.A. Ahmadova, S.F. Hashimzade, E. Imanov, H.G. Khasiyev, N.K. Karimova, F.I. Zubkov, Surface and biocidal properties of gemini cationic surfactants based on propoxylated 1,6-diaminohexane and alkyl bromides, J. Surfactants Deterg. (2021), 12506, https://doi.org/10.1002/jsde.12506 jsde.
[42] Y. Gu, M. Zhou, X. Wang, H. Tu, Y. Yang, Y. Zhao, Preparation and performance evaluation of sulfate-quaternary ammonium Gemini surfactant, J. Mol. Liq. 343 (2021), 117665, https://doi.org/10.1016/j.molliq.2021.117665.
[43] A. Valls, B. Altava, V. Aseyev, E. García-Verdugo, S.V. Luis, Imidazolium based gemini amphiphiles derived from L-valine. Structural elements and surfactant properties, J. Mol. Liq. 341 (2021), 117434, https://doi.org/10.1016/j.molliq.2021.117434.
[44] A.R. Ahmady, P. Hosseinzadeh, A. Solouk, S. Akbari, A.M. Szulc, B.E. Brycki, Cationic gemini surfactant properties, its potential as a promising bioapplication candidate, and strategies for improving its biocompatibility: a review, Adv. Colloid Interface Sci. 299 (2022), 102581, https://doi.org/10.1016/j.cis.2021.102581.
[45] Brycki, B.; Szulc, A. Gemini surfactants as corrosion inhibitors. A review. J. Mol. Liq. 2021, 344, doi:10.1016/j.molliq.2021.117686.
[46] M. Muñoz-Úbeda, M. Semenzato, A. Franco-Romero, E. Junquera, E. Aicart, L. Scorrano, I. López-Montero, Transgene expression in mice of the Opa1 mitochondrial transmembrane protein through bicontinuous cubic lipoplexes containing gemini imidazolium surfactants, J. Nanobiotechnology 19 (2021) 1–17, https://doi.org/10.1186/s12951-021-01167-x.
[47] W. Andrzejewska, Z. Pietralik, M. Skupin, M. Kozak, Structural studies of the formation of lipoplexes between siRNA and selected bis-imidazolium gemini surfactants, Colloids Surfaces B Biointerfaces 146 (2016) 598–606, https://doi.org/10.1016/j.colsurfb.2016.06.062.
[48] R. Bhattarai, T. Sutradhar, B. Roy, P. Guha, P. Chettri, A.K. Mandal, A.G. Bykov, A.V. Akentiev, B.A. Noskov, A.K. Panda, Double-tailed cystine derivatives as novel substitutes of phospholipids with special reference to liposomes, J. Phys. Chem. B 120 (2016) 10744–10756, https://doi.org/10.1021/acs.jpcb.6b06413.
[49] R.V. Pavlov, G.A. Gaynanova, D.A. Kuznetsova, L.A. Vasileva, I.V. Zueva, A.S. Sapunova, D.N. Buzyurova, V.M. Babaev, A.D. Voloshina, S.S. Lukashenko, et al., Biomedical potentialities of cationic geminis as modulating agents of liposome in drug delivery across biological barriers and cellular uptake, Int. J. Pharm. 587 (2020), 119640, https://doi.org/10.1016/j.ijpharm.2020.119640.
[50] A.B. Mirgorodskaya, E.I. Yackevich, S.S. Lukashenko, L.Y. Zakharova, A.I. Konovalov, Solubilization and catalytic behavior of micellar system based on gemini surfactant with hydroxyalkylated head group, J. Mol. Liq. 169 (2012) 106–109, https://doi.org/10.1016/j.molliq.2012.02.012.
[51] M. Borse, V. Sharma, V.K. Aswal, P.S. Goyal, S. Devi, Effect of head group polarity and spacer chain length on the aggregation properties of gemini surfactants in an aquatic environment, J. Colloid Interface Sci. 284 (2005) 282–288, https://doi.org/10.1016/j.jcis.2004.10.008.
[52] M.J. Rosen, Adsorption of surface-active agents at interfaces: the electrical double layer, Surfactants Interfacial Phenom (2012) 34–104, https://doi.org/10.1002/0471670561.ch2.
[53] Milton J. Rosen, J.T. Kunjappu, micelle formation by surfactants, in: Surfactants and Interfacial Phenomena, John Wiley & Sons, Inc., Hoboken, NJ, USA, 2012, pp. 105–177.
[54] R. Zana, Critical micellization concentration of surfactants in aqueous solution and free energy of micellization, Langmuir 12 (1996) 1208–1211, https://doi.org/10.1021/la950691q.
[55] J. Aguiar, P. Carpena, J.A. Molina-Bolivar, C. Carnero Ruiz, On the determination of the critical micelle concentration by the pyrene 1:3 ratio method, J. Colloid Interface Sci. 258 (2003) 116–122, https://doi.org/10.1016/S0021-9797(02)00082-6.
[56] A.D. Voloshina, V.E. Semenov, A.S. Strobykina, N.V. Kulik, E.S. Krylova, V.V. Zobov, V.S. Reznik, Synthesis and antimicrobial and toxic properties of novel 1,3-bis(alkyl)-6-methyluracil derivatives containing 1,2,3- and 1,2,4-triazolium fragments, Russ. J. Bioorganic Chem. 43 (2017) 170–176, https://doi.org/10.1134/S1068162017020170.
[57] F.M. Menger, J.S. Keiper, Gemini surfactants, Angew. Chemie - Int. Ed. 39 (2000) 1906–1920, https://doi.org/10.1002/1521-3773(20000602)39:11<1906::AID-ANIE1906>3.0.CO;2-Q.
[58] E.P. Zhiltsova, T.N. Pashirova, R.R. Kashapov, N.K. Gaisin, O.I. Gnezdilov, S.S. Lukashenko, A.D. Voloshina, N.V. Kulik, V.V. Zobov, L.Y. Zakharova, et al., Alkylated 1,4-diazabicyclo[2.2.2]octanes: self-association, catalytic properties, and biological activity, Russ. Chem. Bull. 61 (2012) 113–120, https://doi.org/10.1007/s11172-012-0016-7.
[59] M.L. Briuglia, C. Rotella, A. McFarlane, D.A. Lamprou, Influence of cholesterol on liposome stability and on in vitro drug release, Drug Deliv. Transl. Res. 5 (2015) 231–242, https://doi.org/10.1007/s13346-015-0220-8.
[60] C. Kirby, J. Clarke, G. Gregoriadis, Effect of the cholesterol content of small unilamellar liposomes on their stability in vivo and in vitro, Biochem. J. 186 (1980) 591–598, https://doi.org/10.1042/bj1860591.
[61] X. Li, D. Chen, C. Le, C. Zhu, Y. Gan, L. Hovgaard, M. Yang, Novel mucus-penetrating liposomes as a potential oral drug delivery system: preparation, in vitro characterization, and enhanced cellular uptake, Int. J. Nanomedicine 6 (2011) 3151–3162.

[62] C. Guo, F. Cui, M. Li, F. Li, X. Wu, Enhanced corneal permeation of coumarin-6 using nanoliposomes containing dipotassium glycyrrhizinate: in vitro mechanism and in vivo permeation evaluation, RSC Adv 5 (2015) 75636–75647, https://doi.org/10.1039/c5ra13830b.
[63] X. Sun, F. Li, Y. Wang, W. Liang, Cellular uptake and elimination of lipophilic drug delivered by nanocarriers, Pharmazie 65 (2010) 737–742, https://doi.org/10.1691/ph.2010.0099.
[64] S. Pretor, J. Bartels, T. Lorenz, K. Dahl, J.H. Finke, G. Peterat, R. Krull, A.T. Al-Halhouli, A. Dietzel, S. Büttgenbach, et al., Cellular uptake of coumarin-6 under microfluidic conditions into HCE-T cells from nanoscale formulations, Mol. Pharm. 12 (2015) 34–45, https://doi.org/10.1021/mp500401t.
[65] X. Feng, H. Liu, J. Pan, Y. Xiong, X. Zhu, X. Yan, Y. Duan, Y. Huang, Liposome-encapsulated tiancimycin a is active against melanoma and metastatic breast tumors: the effect of cRGD modification of the liposomal carrier and tiancimycin a dose on drug activity and toxicity, Mol. Pharm. 19 (2022) 1078–1090, https://doi.org/10.1021/acs.molpharmaceut.1c00753.
[66] D.A. Kuznetsova, L.A. Vasileva, G.A. Gaynanova, R.V. Pavlov, A.S. Sapunova, A.D. Voloshina, G.V. Sibgatullina, D.V. Samigullin, K.A. Petrov, L.Y. Zakharova, et al., Comparative study of cationic liposomes modified with triphenylphosphonium and imidazolium surfactants for mitochondrial delivery, J. Mol. Liq. 330 (2021), 115703, https://doi.org/10.1016/j.molliq.2021.115703.
[67] E.A. Burilova, T.N. Pashirova, I.V. Zueva, E.M. Gibadullina, S.V. Lushchekina, A.S. Sapunova, R.M. Kayumova, A.M. Rogov, V.G. Evtjugin, I.A. Sudakov, et al., Bi-functional sterically hindered phenol lipid-based delivery systems as potential multi-target agents against Alzheimer's disease: via an intranasal route, Nanoscale 12 (2020) 13757–13770, https://doi.org/10.1039/d0nr04037a.
[68] P. Bakardzhiev, A. Forys, B. Trzebicka, T. Andreeva, S. Rangelov, Unprecedented formation of sterically stabilized phospholipid liposomes of cuboidal morphology, Nanoscale 13 (2021) 15210–15214, https://doi.org/10.1039/d1nr02856a.
[69] N. Takahashi, K. Higashi, K. Ueda, K. Yamamoto, K. Moribe, Determination of nonspherical morphology of doxorubicin-loaded liposomes by atomic force microscopy, J. Pharm. Sci. 107 (2018) 717–726, https://doi.org/10.1016/j.xphs.2017.10.009.
[70] C.K. Wong, M.H. Stenzel, P. Thordarson, Non-spherical polymersomes: formation and characterization, Chem. Soc. Rev. 48 (2019) 4019–4035, https://doi.org/10.1039/c8cs00856f.
[71] F. Neuhaus, D. Mueller, R. Tanasescu, S. Balog, T. Ishikawa, G. Brezesinski, A. Zumbuehl, Vesicle origami: cuboid phospholipid vesicles formed by template-free self-assembly, Angew. Chemie - Int. Ed. 56 (2017) 6515–6518, https://doi.org/10.1002/anie.201701634.
[72] J.A.S. Almeida, E.F. Marques, A.S. Jurado, A.A.C.C. Pais, The effect of cationic gemini surfactants upon lipid membranes. An experimental and molecular dynamics simulation study, Phys. Chem. Chem. Phys. 12 (2010) 14462–14476, https://doi.org/10.1039/c0cp00950d.
[73] S.K. Amerkhanova, A.D. Voloshina, A.B. Mirgorodskaya, A.P. Lyubina, D.A. Kuznetsova, R.A. Kushnazarova, V.A. Mikhailov, L.Y. Zakharova, Antimicrobial properties and cytotoxic effect of imidazolium geminis with tunable hydrophobicity, Int. J. Mol. Sci. (2021) 22, https://doi.org/10.3390/ijms222313148.
[74] H.L. Zhu, Z.Y. Hu, X.M. Ma, J.L. Wang, D.L. Cao, Synthesis, surface and antimicrobial activities of cationic gemini surfactants with semi-rigid spacers, J. Surfactants Deterg. 19 (2016) 265–274, https://doi.org/10.1007/s11743-015-1777-4.
[75] B.E. Brycki, A. Szulc, I. Kowalczyk, A. Koziróg, E. Sobolewska, Antimicrobial activity of gemini surfactants with ether group in the spacer part, Molecules (2021) 26, https://doi.org/10.3390/molecules26195759.
[76] P. Balgavý, F. Devínsky, Cut-off effects in biological activities of surfactants, Adv. Colloid Interface Sci. 66 (1996) 23–63, https://doi.org/10.1016/0001-8686(96)00295-3.
[77] F. Versluis, J. Voskuhl, B. Van Kolck, H. Zope, M. Bremmer, T. Albregtse, A. Kros, In situ modification of plain liposomes with lipidated coiled coil forming peptides induces membrane fusion, J. Am. Chem. Soc. 135 (2013) 8057–8062, https://doi.org/10.1021/ja4031227.
[78] R. Münter, M. Bak, E. Christensen, P.J. Kempen, J.B. Larsen, K. Kristensen, L. Parhamifar, T.L. Andresen, Mechanisms of selective monocyte targeting by liposomes functionalized with a cationic, arginine-rich lipopeptide, Acta Biomater 144 (2022) 96–108, https://doi.org/10.1016/j.actbio.2022.03.029.